Human Molecular Genetics, 2015, Vol. 24, No. 22 6492–6504

doi: 10.1093/hmg/ddv358
Advance Access Publication Date: 10 September 2015
Original Article

ORIGINAL ARTICLE

Mitochondrial ATP synthase activity is impaired by suppressed *O*-GlcNAcylation in Alzheimer's disease

Moon-Yong Cha[1,†], Hyun Jin Cho[1,†], Chaeyoung Kim[6], Yang Ouk Jung[2], Min Jueng Kang[3], Melissa E. Murray[6], Hyun Seok Hong[4], Young-Joo Choi[1], Heesun Choi[1], Dong Kyu Kim[1], Hyunjung Choi[1], Jisoo Kim[1], Dennis W. Dickson[6], Hyun Kyu Song[2], Jin Won Cho[5], Eugene C. Yi[3], Jungsu Kim[6], Seok Min Jin[1,*] and Inhee Mook-Jung[1,*]

[1]Department of Biochemistry and Biomedical Sciences, Seoul National University, College of Medicine, Seoul, Korea, [2]Department of Life Sciences, Korea University, Seoul, Korea, [3]Department of Molecular Medicine and Biopharmaceutical Sciences, Graduate School of Convergence Science and Technology, School of Medicine and School of Pharmacy, Seoul National University, Seoul, Korea, [4]Medifron-DBT, Inc., Gyeonggi-do, Korea, [5]Department of Integrated OMICS for Biomedical Science, Graduate School, Yonsei University, Seodaemun-gu, Seoul, Korea and [6]Department of Neuroscience, Mayo Clinic College of Medicine, Jacksonville, FL 32224, USA

*To whom correspondence should be addressed. Tel: +8 227408245; Fax: +8 2236727352; Email: inhee@snu.ac.kr (Inhee Mook-Jung), Tel: +8 2236687637; Fax: +8 2236727352; Email: neurocom@snu.ac.kr (Seok Min Jin)

Abstract

Glycosylation with *O*-linked β-*N*-acetylglucosamine (*O*-GlcNAc) is one of the protein glycosylations affecting various intracellular events. However, the role of *O*-GlcNAcylation in neurodegenerative diseases such as Alzheimer's disease (AD) is poorly understood. Mitochondrial adenosine 5′-triphosphate (ATP) synthase is a multiprotein complex that synthesizes ATP from ADP and P_i. Here, we found that ATP synthase subunit α (ATP5A) was *O*-GlcNAcylated at Thr432 and ATP5A *O*-GlcNAcylation was decreased in the brains of AD patients and transgenic mouse model, as well as Aβ-treated cells. Indeed, Aβ bound to ATP synthase directly and reduced the *O*-GlcNAcylation of ATP5A by inhibition of direct interaction between ATP5A and mitochondrial *O*-GlcNAc transferase, resulting in decreased ATP production and ATPase activity. Furthermore, treatment of *O*-GlcNAcase inhibitor rescued the Aβ-induced impairment in ATP production and ATPase activity. These results indicate that Aβ-mediated reduction of ATP synthase activity in AD pathology results from direct binding between Aβ and ATP synthase and inhibition of *O*-GlcNAcylation of Thr432 residue on ATP5A.

Introduction

Alzheimer's disease (AD) is the most prevalent neurodegenerative disease. Although it has been studied for more than a century, the molecular bases for its pathogenesis are still far from being clearly understood. Accordingly, no cure or prevention is yet available. This deleterious brain disease is characterized by two remarkable pathologies known as senile plaques and neurofibrillary tangles, which correspond to extracellular aggregates of Aβ peptide and intracellular inclusions of hyperphosphorylated tau, respectively (1–3). Since the development of the fluorodeoxyglucose positron emission tomography (FDG-PET) technique, another important feature of AD has been revealed, i.e. perturbed cerebral glucose

[†]These authors contributed equally to the work.

Received: June 2, 2015. **Revised:** August 17, 2015. **Accepted:** September 1, 2015

© The Author 2015. Published by Oxford University Press. All rights reserved. For Permissions, please email: journals.permissions@oup.com

metabolism. A recent study has suggested that abnormal FDG-PET precedes other pathological symptoms in patients at risk of developing AD (4). Indeed, abnormal cerebral glucose metabolism is one of the parameters used to clinically diagnose AD.

At the cellular level, the tricarboxylic acid (TCA) cycle is the main catabolic process to use products of glucose metabolism in the mitochondrial matrix, and provides NADH and succinate to the electron transport chain (ETC) in the mitochondrial inner membrane (5,6). The ETC generates a proton gradient across the mitochondrial inner membrane using NADH and succinate fed from the TCA cycle as redox carriers. Using this proton gradient as a motive force, the last component of the ETC (complex V, mitochondrial F_oF_1-ATP synthase) produces the cellular energy carrier, adenosine 5′-triphosphate (ATP) (7–9). Substantial evidence indicates that mitochondrial dysfunction is one of the consistent features of AD and occurs in the early stages of disease development (10–13). In the postmortem brains of AD patients, the enzyme activities of TCA cycle and the ETC are altered (14–16). Moreover, it was recently reported that ATP synthase activity and ATP levels are reduced in the brains of AD patients (17). In an AD mouse model that produces large amounts of human amyloid beta (Aβ), mitochondrial dysfunction is apparent before plaque formation (18), and cultured embryonic hippocampal neurons from an AD mouse model show decreased respiration and increased glycolysis (19). In spite of the controversy concerning the presence of Aβ in mitochondria, this has also been demonstrated. Aβ peptides are imported into the mitochondria through mitochondrial protein import machinery and interact with matrix proteins such as alcohol dehydrogenase [ABAD; also known as hydroxysteroid (17-β) dehydrogenase 10 (HSD17B10) and cyclophilin D (also known as peptidylprolyl isomerase D (PPID)] (20,21).

O-GlcNAcylation is a post-translational modification that adds a single *N*-acetylglucosamine (GlcNAc) moiety to specific serine or threonine residues on target proteins via an *O*-glycosidic bond (22,23). In recent years, many researchers have focused on this unique form of glycosylation due to the fact that *O*-GlcNAcylation can compete with the phosphorylation of serine or threonine residues and thus affect various cellular signaling events (24,25). In addition, *O*-GlcNAcylation is regarded as a glucose sensor, as uridine diphosphate-N-acetylglucosamine (UDP-GlcNAc), which supplies the GlcNAc moiety for the reaction, is produced from extracellular glucose via the hexosamine biosynthetic pathway. Accordingly, the *O*-GlcNAcylation of proteins is diminished in brain extracts from AD patients who have perturbed glucose metabolism (26,27). Also, some studies suggest enhanced *O*-GlcNAc pathway attenuates Aβ generation (26,28). The transfer of the GlcNAc moiety from UDP-GlcNAc to the target protein is mediated by *O*-GlcNAc transferase (OGT), whereas *O*-GlcNAcase (OGA) mediates removal of the sugar moiety. OGT exists as two isoforms, nucleocytoplasmic OGT (ncOGT) and mitochondrial OGT (mOGT), generated by alternative splicing of a single gene. Compared with the ncOGT-mediated modification of nuclear/cytosolic proteins, only limited information is available so far regarding the identity of mitochondrial proteins modified by mOGT.

We examined the effect of Aβ on *O*-GlcNAcylation of mitochondrial proteins and found that the *O*-GlcNAcylation of ATP5A was reduced and ATP synthase activity was decreased in brains from a transgenic AD mouse model (5 × FAD Tg; Tg6799), as well as in mammalian cell lines and primary cortical neurons when these were treated with Aβ. Molecular dynamics (MD) analysis revealed that Aβ bound to ATP synthase, and this binding was blocked by *O*-GlcNAcylation of ATP5A, which is resulted from the inhibition of direct interaction between ATP5A and mOGT by Aβ. Indeed, treatment with an OGA inhibitor restored the Aβ-mediated reductions of ATP5A *O*-GlcNAcylation and ATP synthase activity. Based on these results, we demonstrate that direct binding of Aβ to ATP5A reduces ATP synthase activity by inhibition of ATP5A *O*-GlcNAcylation, and that upregulation of *O*-GlcNAcylation ameliorate the deleterious effects of Aβ on ATP synthesis in AD pathological condition.

Results

O-GlcNAcylation of ATP5A and ATP synthase activity are decreased in the cortex of an AD mouse model

To investigate the *O*-GlcNAcyl modification of the mitochondrial proteome, we pulled down *O*-GlcNAcylated proteins from a crude mitochondrial fraction of mouse cortex using agarose beads conjugated with succinylated wheat germ agglutinin (sWGA), a modified lectin known to specifically bind to GlcNAcylated proteins (29). *O*-GlcNAcylated proteins purified from the mitochondrial fraction were eluted and then identified using liquid chromatography coupled with tandem mass spectrometry (LC-MS/MS) (Supplementary Material, Table S2). We also tried to identify mitochondrial proteins that interact with Aβ. To this end, a mitochondria-enriched fraction was incubated with biotin-conjugated Aβ and then the bound proteins were pulled down using streptavidin-agarose. Eluted Aβ-binding proteins were identified using LC-MS/MS. One of the prominent candidates for *O*-GlcNAcylation as well as Aβ-binding in mitochondria was ATP5A (Supplementary Material, Table S3). Based on the results from the proteomic approach, we questioned whether Aβ affects the extent of *O*-GlcNAcylation of ATP5A and the activity of the whole enzyme in the pathological conditions. To answer these questions, we first analyzed the level of *O*-GlcNAcylation of ATP5A in the entorhinal cortex of AD patients reported to have decreased ATP synthase activity and ATP level (Terni *et al*, 2010) using sWGA pull-down assay. Interestingly, the amount of *O*-GlcNAcylated ATP5A was significantly reduced in the brains of AD patients without any changes of total amount of ATP5A protein (Fig. 1A and B). In line with this result, the amount of *O*-GlcNAcylated ATP5A was also dramatically decreased in the brains of Tg6799 mice (Tg) compared with littermate (LT) brains (Fig. 1C and D). In this setting, the overall pattern of protein *O*-GlcNAcylation and the protein levels of enzymes responsible for *O*-GlcNAcyl protein modifications, OGT and OGA, were not altered, indicating that the level of *O*-GlcNAcylation of ATP5A is specifically altered in the presence of Aβ in the pathological condition (Fig. 1C). The next question was whether this change in the epigenetic modification of ATP5A results in a functional impairment in the enzymatic activity of ATP synthase. As shown in Figure 1E, the level of ATP, which is the end-product of ATP synthase in the normal condition, was also substantially abrogated in cortical extracts from Tg6799 mice (Tg), suggesting the possibility that *O*-GlcNAcyl modification of the ATP synthase subunit affected the activity of the holoenzyme. As the overproduction of Aβ is known to exert many deleterious effects on various essential cellular events, we needed to address whether reduced ATP synthase activity was related to the *O*-GlcNAcyl modification of ATP5A.

ATP5A is O-GlcNAcylated in mammalian cells and primary neurons

First, we tested the specificity of the sWGA pull-down assay for *O*-GlcNAcylated proteins and *O*-GlcNAcylation of ATP5A in cultured mammalian cells (Fig. 2A). ATP5A was pulled down from whole cell extracts of HeLa cells using sWGA-conjugated agarose

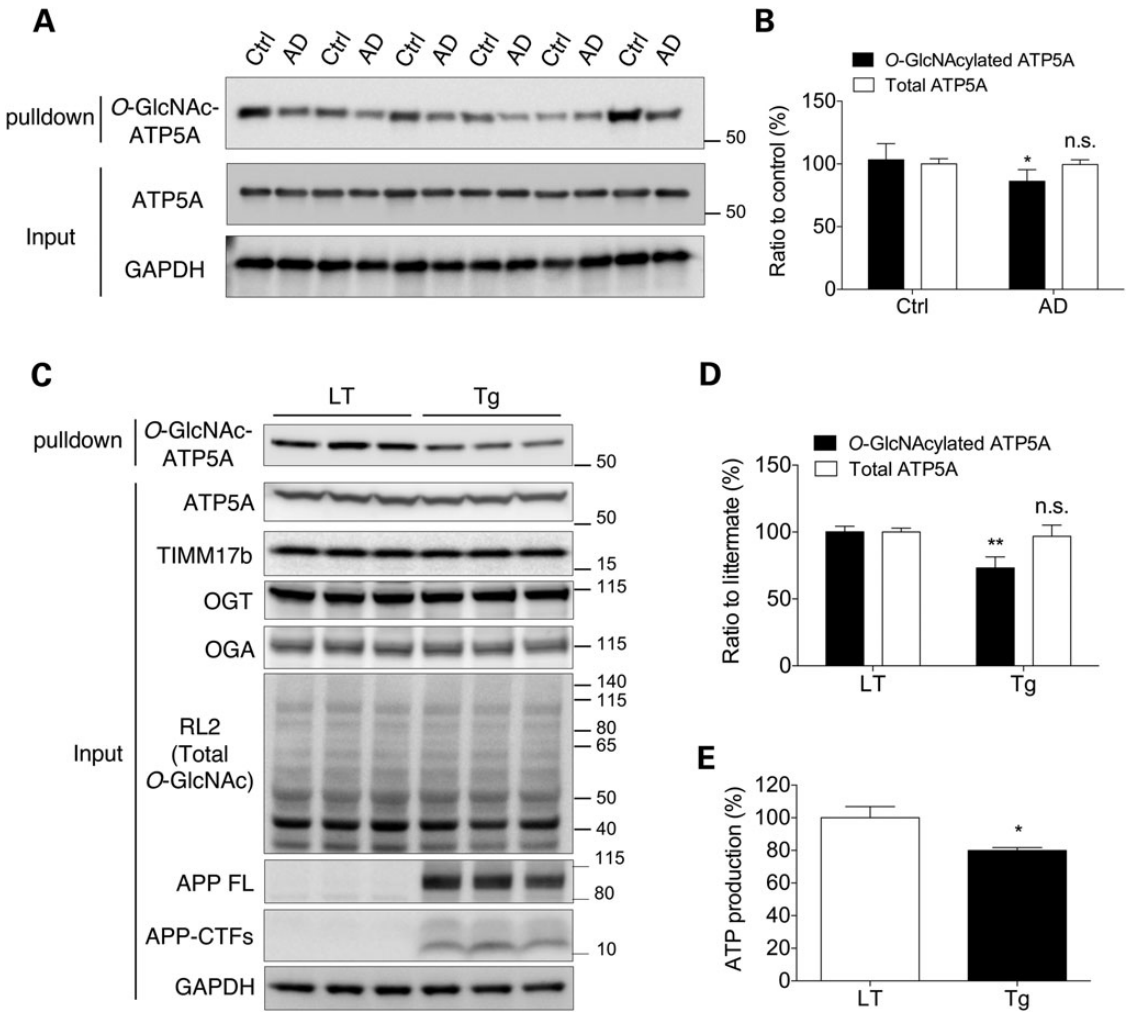

Figure 1. Decreased O-GlcNAcylation and ATP synthase activity in AD model brains. (**A**) O-GlcNAcylated ATP5A in the brains from AD patients (AD) and controls (Ctrl). Total proteins were extracted from the dissected entorhinal cortex of AD and control brains to determine the expression levels of the indicated proteins. In the top panel, total O-GlcNAcylated proteins were pulled down with sWGA-agarose beads from entorhinal cortical lysates and the level of O-GlcNAc-ATP5A was then assessed by western blotting with an anti-ATP5A mAb ($n = 6$ per group). (**B**) The intensities of total ATP5A and O-GlcNAc-ATP5A in (A) were analyzed using densitometry and the level of O-GlcNAc-ATP5A was normalized to ATP5A. (**C**) O-GlcNAcylated ATP5A in the Tg6799 (Tg) mouse brain. Total proteins were extracted from the dissected cortices of Tg6799 mice and LTs to determine the expression levels of the indicated proteins. In the top panel, total O-GlcNAcylated proteins were pulled down with sWGA-agarose beads from cortex lysates and the level of O-GlcNAc-ATP5A was then assessed by western blotting with an anti-ATP5A mAb ($n = 5$ per group). (**D**) The intensities of total ATP5A and O-GlcNAc-ATP5A in (C) were analyzed using densitometry and the level of O-GlcNAc-ATP5A was normalized to ATP5A. (**E**) ATP production was measured in brain extracts from Tg6799 mice (Tg) and LTs ($n = 5$ per group). The results were represented as mean ± standard error from three independent experiments. $^{**}P < 0.01$; $^{*}P < 0.05$; n.s.: non-significant.

beads, but not using non-conjugated agarose beads. The pull down was completely abolished by preincubation of the sWGA-conjugated agarose beads with an excess of free GlcNAc. To confirm that the pull down of ATP5A was associated with GlcNAcylated protein residues, we treated the sample proteins or the pull-down fraction with β-D-*N*-acetyl-hexosaminidase (β-HEX), an O-GlcNAc-specific exoglycosidase that catalyzes the hydrolysis of β-D-*N*-acetylglucosamine residues (Fig. 2B). Treatment of the whole cell lysate with β-HEX remarkably decreased the intensity of immunoreactive bands that were specific for RL2, a mAb for O-GlcNAcylated proteins, confirming the effect of the β-HEX treatment (Fig. 2B, left panel). When the sWGA-agarose pulled down fraction was treated with β-HEX and then agarose beads and supernatants were separated by centrifugation, ATP5A immunoreactivity was remarkably diminished in the bead fraction (GlcNAc-sWGA-agarose) and instead appeared in the supernatant fraction, indicating that the binding between ATP5A and sWGA-agarose beads was mediated by the GlcNAcyl modification of ATP5A (Fig. 2B, right panel). Then, we tested whether the modification of ATP5A was affected by chemical or genetic modulation of the O-GlcNAcylation machinery. The results showed that treatment with ST045849 (ST, 25 μM, 24 h), an OGT inhibitor, remarkably decreased the level of O-GlcNAcylation of ATP5A as well as whole proteins (RL2 immunoreactive bands) without affecting the total ATP5A level (Fig. 2C, left column). By contrast, treatment with Thiamet G (ThG, 3 μM, 24 h), an OGA inhibitor, increased the O-GlcNAcylation level of total proteins, but not the level of O-GlcNAcylated ATP5A (Fig. 2C, right column), suggesting that OGT activity is far more dominant than OGA activity, at least in the mitochondria of normally growing cells. These events were also confirmed using cultured primary cortical neurons. Chemical inhibition of OGT or OGA modulated the O-GlcNAcylation of total proteins in neurons more effectively (compare RL2 immunoreactive bands between Fig. 2C and D). The

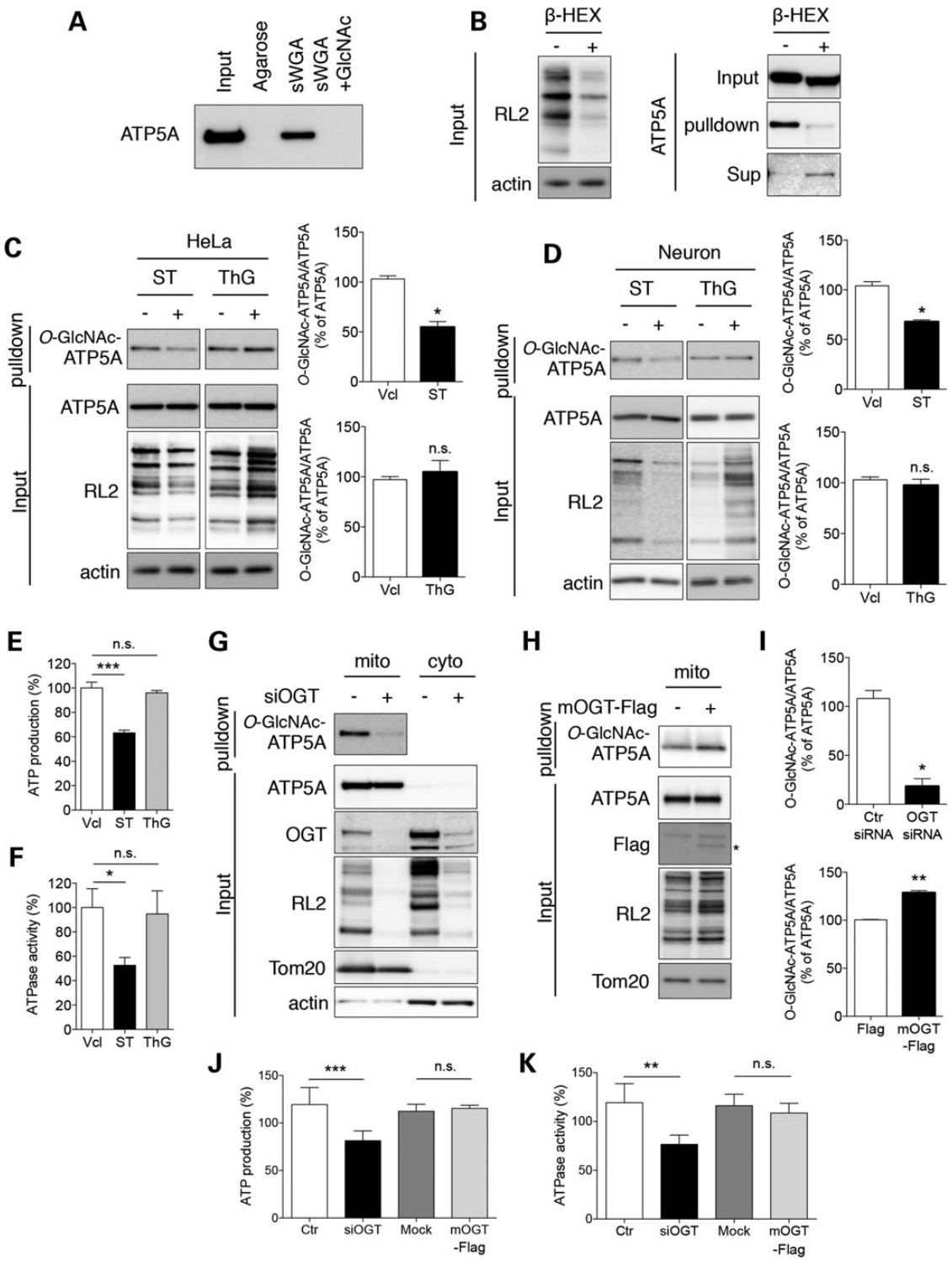

Figure 2. O-GlcNAcylation of ATP5A in cultured cells. **(A)** Specificity of sWGA-agarose pull-down in a competition assay. All O-GlcNAcylated proteins were pulled down from total protein extracts (300 μg) of HeLa cells with agarose or sWGA-conjugated agarose in the presence or absence of free *N*-acetylglucosamine (GlcNAc) as a competitor. The level of ATP5A was measured by immunoblotting. **(B)** Specificity of sWGA-agarose pull-down by treatment with β-hexosaminidase (β-HEX). Total protein extracts (20 μg; left panel) or O-GlcNAc proteins pulled down with sWGA-agarose (right panel) were treated with β-HEX and analyzed for the total levels of O-GlcNAcylation (left panel) or O-GlcNAc-ATP5A in the indicated fractions (right panel) by western blotting. β-actin or total ATP5A were included as loading controls for each fraction. **(C)** Effect of changes of the O-GlcNAcylation machinery on O-GlcNAc-ATP5A in HeLa cells. HeLa cells were treated with an OGT inhibitor (ST045849; ST, 25 μM) or OGA inhibitor (Thiamet G; ThG, 1 μM) for 24 h. Samples or sWGA-agarose pull-down fractions were analyzed by western blotting with the indicated antibodies. Bar graphs show densitometric quantification of O-GlcNAcylated ATP5A in HeLa cells. **(D)** Effect of changes of the O-GlcNAcylation machinery on O-GlcNAc-ATP5A in primary cultured neurons. Primary cortical neurons were cultured from the brains of B6/SJL mice and treated as in (C). The level of O-GlcNAc-ATP5A was detected by western blotting. Bar graphs show densitometric quantification of O-GlcNAcylated ATP5A in neurons. **(E, F)** ATP production (E) and ATPase activity (F) from extracts of HeLa cell treated with OGA or OGT inhibitor. HeLa cells were incubated in the presence or absence of OGA or OGT inhibitor (1 μM ThG or

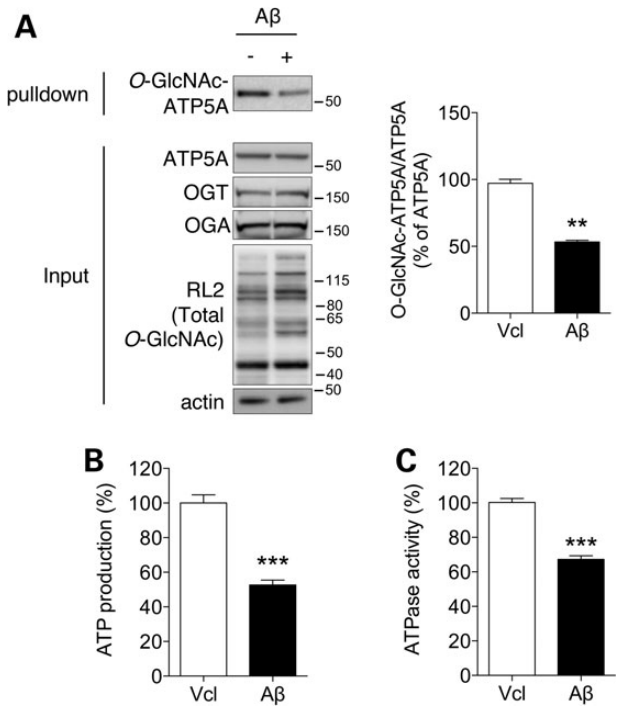

Figure 3. Effect of Aβ on *O*-GlcNAcylation and the function of ATP synthase. HeLa cells were treated with vehicle (Vcl) or Aβ (3 μM, 24 h) and whole cell lysates were prepared. The expression levels of the indicated proteins (**A**), ATP production (**B**) and ATPase activity (**C**) were measured by western blotting or *in vitro* assays ($n = 3$ per group). Bar graph in (A) shows densitometric quantification of *O*-GlcNAcylated ATP5A in HeLa cells. The results were represented as mean ± standard error from three independent experiments. ***$P < 0.001$; **$P < 0.01$; n.s.: non-significant.

O-GlcNAcylation of ATP5A was accordingly inhibited by treatment with ST but not ThG, suggesting that the *O*-GlcNAcylation of ATP5A could be one of the general mechanisms regulating ATP synthase activity in mammalian systems (Fig. 2D). We addressed whether changes in the *O*-GlcNAcylation of ATP5A by ThG and ST affected the enzymatic activity of ATP synthase (Fig. 2E and F). Consistent with the *O*-GlcNAcylation of ATP5A, ThG had no effect on ATP production and ATPase activity, but ST significantly decreased both ATP production and ATPase activity. Also, the knockdown of OGT greatly ameliorated the *O*-GlcNAcylation of ATP5A while whole proteins revealed no alteration in the total amount of ATP5A protein in the mitochondrial fraction (Fig. 2G and I). We overexpressed a mitochondrial OGT construct (FLAG-mOGT) to confirm the *O*-GlcNAcylation of ATP5A in mitochondria. As expected, overexpression of mOGT led to up-regulation of ATP5A *O*-GlcNAcylation (Fig. 2H and I). Furthermore, siRNA-mediated OGT knockdown led to down-regulations of ATP production and ATPase activity (Fig. 2J and K). Interestingly, overexpression of mOGT showed no significant alterations in ATP production and ATPase activity, implicating that excessive *O*-GlcNAcylation of ATP5A has no effect on ATPase activity in normal condition. Collectively, these data reveal that ATP5A is functionally regulated by *O*-GlcNAcylation.

Aβ abrogated the O-GlcNAcylation of ATP5A

Since the protein extracts from Tg6799 mouse cortex showed reduced levels of *O*-GlcNAcylated ATP5A in Figure 1, we checked whether an excess of Aβ, implicating AD-like pathological condition, affects the *O*-GlcNAcylation of ATP5A in mamalian cells (Fig. 3A). As in the cortex of the AD mouse model, Aβ-treated cells revealed a reduction in *O*-GlcNAcylated ATP5A without a change in the protein levels of OGA, OGT and ATP5A, even though the *O*-GlcNAcylation pattern of the total proteins was slightly increased. Furthermore, ATP production and ATP hydrolyzing activity were also decreased by Aβ treatment, indicating that Aβ inhibits ATP synthase activity in both directions (Fig. 3B and C).

Thr_{432} in ATP5A is O-GlcNAcylated

We used mass spectrometry to map the *O*-GlcNAcylation sites in ATP5A and found six putative sites (Fig. 4A). To verify *O*-GlcNAcylation on those residues biochemically, mutant constructs were generated by replacing the Ser/Thr residue on each putative ATP5A *O*-GlcNAcylation site with Ala to make it no longer capable of being modified by *O*-GlcNAcylation. When the mutant constructs were expressed in HeLa cells, the T432A mutant presented the significant reduction in the level of *O*-GlcNAcylated ATP5A (Fig. 4B). The LC-MS/MS results for the *O*-GlcNAcylation of the Thr432 residue are shown in Figure 4C. The *O*-GlcNAc-modified AMKQVAGTMK peptide of human ATP5A (residues 425–434) was observed at a $[M + 2H]^{2+}$ mass-to-charge ratio (m/z) of 642.32, which imply that Thr432 residue is *O*-GlcNAcylated. Furthermore, ATP production and ATP hydrolyzing activity were also significantly decreased in ATP5A T432 mutant overexpressing cells (Fig. 4D and E), indicating that Thr432 in ATP5A is functionally *O*-GlcNAcylated.

Aβ inhibits direct interaction between ATP5A and mOGT

To determine whether the *O*-GlcNAcylation of ATP5A was associated with direct binding with mOGT, cells were co-transfected with FLAG-mOGT and ATP5A-GFP constructs. Interestingly, the ATP5A-GFP was co-immunoprecipitated with mOGT (Fig. 5A). Furthermore, the ATP5A T432A mutant having impaired *O*-GlcNAcylation of ATP5A exhibited decreased binding affinity with mOGT (Fig. 5A). We then tried to test whether pathologically excess of Aβ modulates the interaction of mOGT with ATP5A, and found that treatment with Aβ disrupted the interaction between mOGT and ATP5A (Fig. 5B). These data demonstrate that *O*-GlcNAcylation of ATP5A is regulated by its binding affinity with mOGT and pathological treatment of Aβ perturbs the direct interaction of mOGT with ATP5A.

Aβ binding and O-GlcNAcylation happen in close proximity on ATP synthase

The protein levels of OGA and OGT showed no changes in Aβ-treated cells as well as in brain cortical extracts from the AD mouse model having excessive amount of Aβ (Figs. 1A and 3A). Our next question was how Aβ specifically modulates the

25 μM ST for 24 h). ATP production was measured as described in Materials and Methods ($n = 3$ per group). (**G**) Effect of OGT knockdown on *O*-GlcNAc-ATP5A in HeLa cells. HeLa cells were transfected with 20 nM siRNA against OGT. After 48 h, cells were fractionated and the mitochondrial and cytosolic fractions were analyzed by western blotting with the indicated antibodies. (**H**) Effect of mOGT overexpression on *O*-GlcNAc-ATP5A in HeLa cells. HeLa cells were transfected with a FLAG-mOGT construct. After 48 h, cells were fractionated and the mitochondrial fraction was analyzed by western blotting with the indicated antibodies. (**I**) Densitometric quantifications of *O*-GlcNAcylated ATP5A levels in OGT knockdown system (G) and mOGT overexpressing cells (H). (**J**, **K**) ATP production (J) and ATPase activity (K) from protein extracts of HeLa cells transfected with siRNA against OGT or FLAG-mOGT construct. ATP production and ATPase activity were measured as described in Materials and Methods ($n = 3$ per group). The results were represented as mean ± standard error from three independent experiments. ***$P < 0.001$; **$P < 0.01$; *$P < 0.05$; n.s.: non-significant.

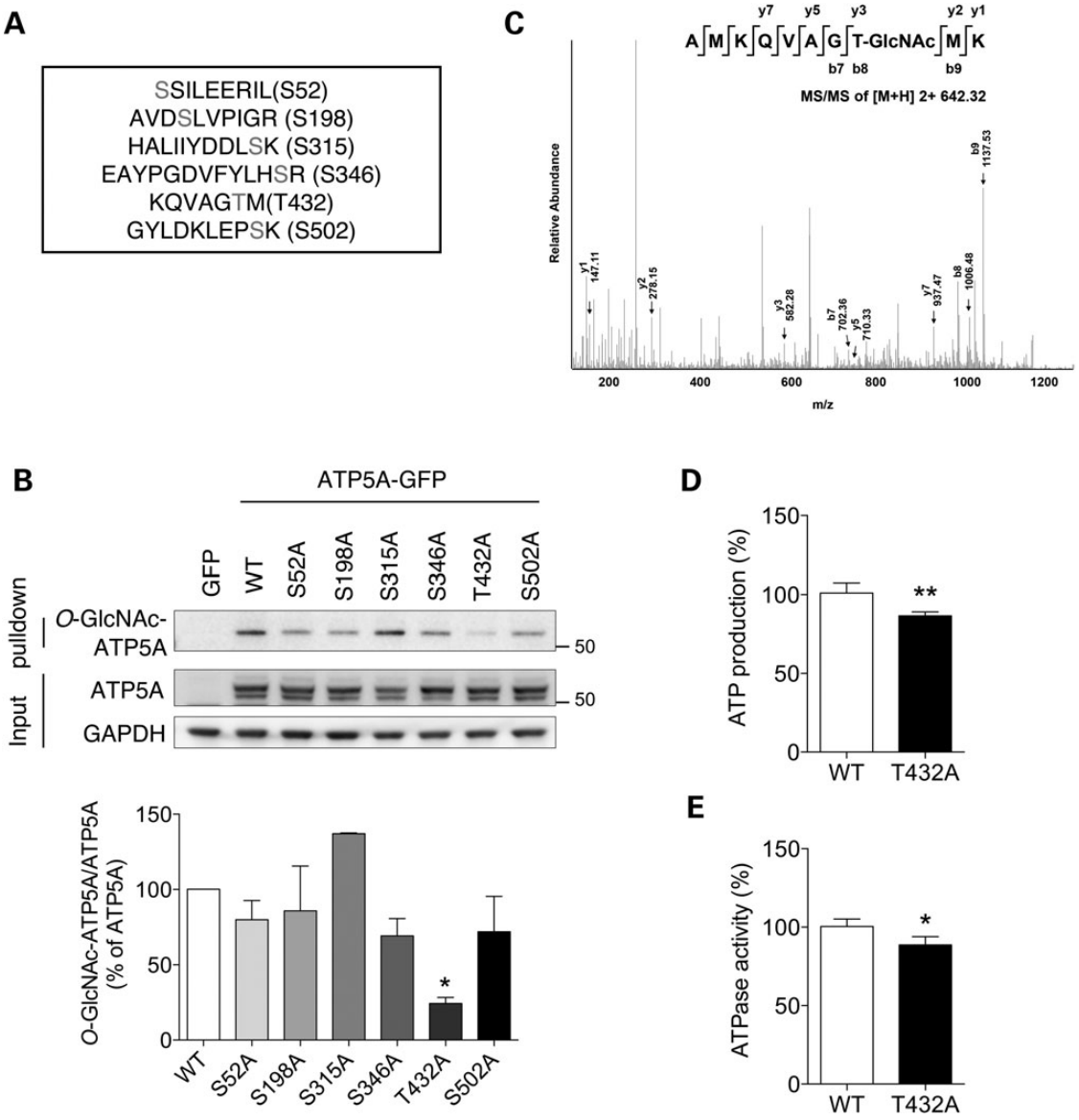

Figure 4. Mapping of the O-GlcNAc modification sites on ATP5A. (**A**) LC-MS/MS result for putative O-GlcNAcylation sites on ATP5A. (**B**) Validation of O-GlcNAcylation on ATP5A through site-directed mutagenesis. Cells were transfected with GFP, WT ATP5A or mutant ATP5A in which putative O-GlcNAcylation sites were replaced with Ala. After 48 h transfection, whole cell lysates were prepared and pulled down with sWGA-agarose beads. O-GlcNAcylated ATP5A was detected by western blotting. Bar graph shows densitometric quantification of O-GlcNAcylated ATP5A in cells. (**C**) O-GlcNAcylation of ATP5A on Thr432. (**D**, **E**) ATP production (D) and ATPase activity (E) from extracts of HeLa cell transfected with ATP5A WT or ATP5A T432 mutant construct (T432A). After 48 h, ATP production and ATPase activity were measured as described in Materials and Methods ($n = 3$ per group). The results were represented as mean ± standard error from three independent experiments. $^{**}P < 0.01$; $^{*}P < 0.05$; n.s.: non-significant.

O-GlcNAcylation of ATP5A. To answer this question, molecular modeling of the O-GlcNAcyl modification of the Thr432 residue was performed in silico. Using the three dimensional structure of bovine ATP5A (PDB ID: 1OHH), we mapped the O-GlcNAc-Thr432 residue and found that the GlcNAc group was exposed to the surface, making it accessible to OGA or OGT (Fig. 6A and B). We then tried a docking simulation using the NMR structures of human $A\beta_{1\text{-}42}$ and bovine ATP synthase (Fig. 6C). Interestingly, it revealed that Aβ could preferentially bind to the pocket between the C-termini of ATP5A and ATP5B, which is close to the O-GlcNAcylation site of ATP5A. This close proximity between the Aβ binding site and the Thr432 residue on ATP synthase suggests the possibility that O-GlcNAcylation of ATP5A and Aβ binding with ATP synthase affect each other. To confirm the result of the docking simulation between ATP synthase and Aβ and also to test the expectations regarding the Aβ binding site biochemically, we produced deletion mutants of ATP5A and ATP5B (ATP synthase subunit β) having no pocket site (30), and an Aβ-expressing construct targeted to the mitochondria by an N-terminal targeting sequence (mito-Aβ) (31). When we overexpressed these constructs in cultured cells, mito-Aβ was co-immunoprecipitated with wild-type (WT) ATP5A and ATP5B but not with the deletion mutants, confirming the location of the binding site for Aβ on ATP synthase in mitochondria (Fig. 6D). Taken together, the binding site of Aβ on ATP5A and O-GlcNAcylation site on ATP5A have close proximity based on docking simulation

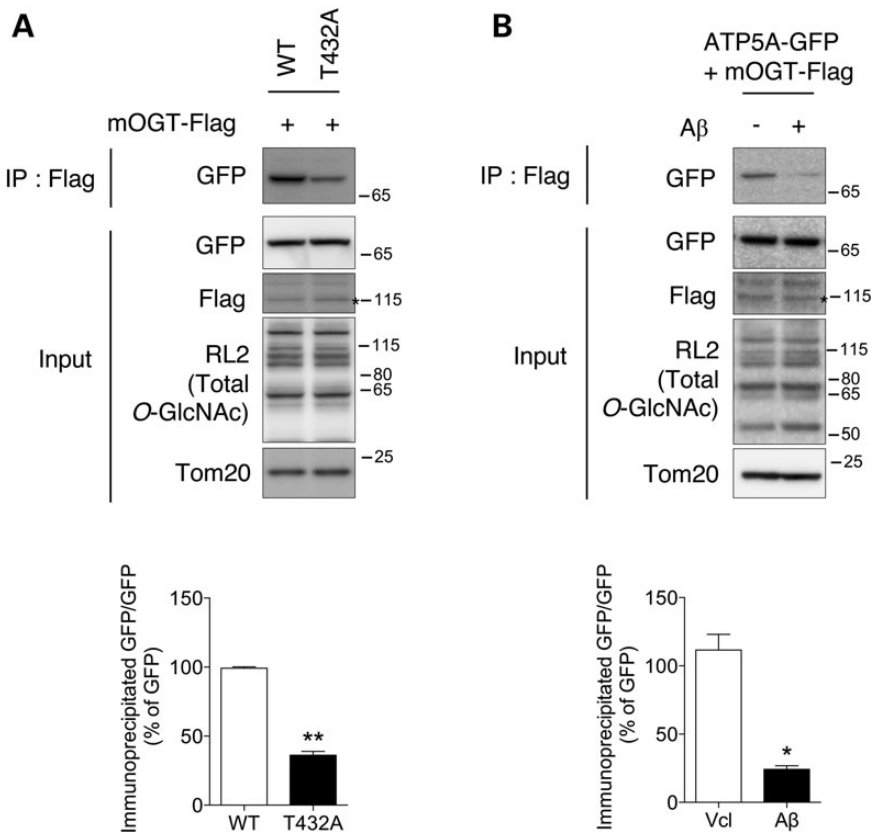

Figure 5. Blocking of the interaction between ATP5A and mOGT by Aβ treatment. (**A**) Co-immunoprecipitation of FLAG-mOGT and ATP5A-GFP. Cells were co-transfected with FLAG-mOGT, ATP5A WT or ATP5A T432 mutant construct (T432A). After 48 h, cells were fractionated and the mitochondrial fraction was analyzed by western blotting with the indicated antibodies. Bar graph shows densitometric quantification of immunoprecipated band. (**B**) Cells overexpressing FLAG-mOGT and ATP5A-GFP were treated with 3 μM Aβ for 48 h. Prepared mitochondrial fraction was analyzed by western blotting with the indicated antibodies. Bar graph shows densitometric quantification of immunoprecipated band. The result was represented as mean ± standard error from three independent experiments. $^{**}P < 0.01$; $^{*}P < 0.05$. Stars indicate overexpressed protein.

experiments even though Aβ binding site on ATP5A is different from O-GlcNAcylation residue on ATP5A.

Up-regulation of O-GlcNAcylation rescued Aβ-reduced ATP5A O-GlcNAcylation and ATP synthase activity

So far, it had been observed that Aβ targeted into the mitochondrial matrix bound to mitochondrial ATP synthase, resulting in the inhibition of α subunit *O*-GlcNAcylation by probable competition between Aβ and mOGT. Next, we verified whether enhanced ATP5A *O*-GlcNAcylation reverse this pathologically excessive Aβ-induced impairments of ATP5A *O*-GlcNAcylation and ATP synthase activity by up-regulation of *O*-GlcNAcylation using ThG treatment (Fig. 7A). As a result, decreased *O*-GlcNAcylation of ATP5A in response to excess of Aβ, implicating the pathological condition, was rescued by ThG treatment, although ThG itself showed no increase in ATP5A *O*-GlcNAcylation in the normal condition, as shown in Figure 2C. This recovery effect was also reproduced in cultured primary cortical neurons as well as other cell line, Chinese hamster ovary (CHO) cells (Fig. 7A). We also tested whether ThG treatment rescue the Aβ-induced inhibition of ATP production and ATPase activity (Fig. 7B and C). As results, treatment with ThG partially but significantly rescued the lowered ATP production and ATPase activity in Aβ-treated cells. Next, we injected ThG into Tg6799 mice (Tg) to confirm the recovery effect of ThG in an *in vivo* system. The *O*-GlcNAcylation level of whole proteins extracted from brain tissue was up-regulated by i.v. injection of ThG. Also, administration of ThG restored the diminished *O*-GlcNAcylated ATP5A levels in Tg6799 mouse brains (Fig. 7D). Furthermore, ThG-injected Tg6799 mice showed restored ATP production, similar to that seen in HeLa cells (Fig. 7E). Taken together, up-regulation of *O*-GlcNAcylation using ThG treatment recovers pathologically excessive Aβ-induced impairments of ATP5A *O*-GlcNAcylation and ATP synthase activity.

Discussion

Disruption of ATP synthesis has detrimental effects on that most essential of cellular events: the demand for energy. It has been known for a long time that a continuous decline in bio-energetic capacity is related to the aging of the mammalian nervous system. It has also been reported that ATP levels and, more recently, ATP synthase activity are decreased in the brains of AD patients (17). However, the underlying mechanisms are still not clear.

One of the possible mechanisms for the deterioration in ATP synthesis in normal aging and AD development could be a change in post-translational modifications on the subunits of ATP synthase. Many post-translational modifications such as nitration, S-nitrosylation, tryptophan oxidation, acetylation and phosphorylation have been reported for the various components of ATP synthase (32–34). *O*-GlcNAcylation is another post-translational

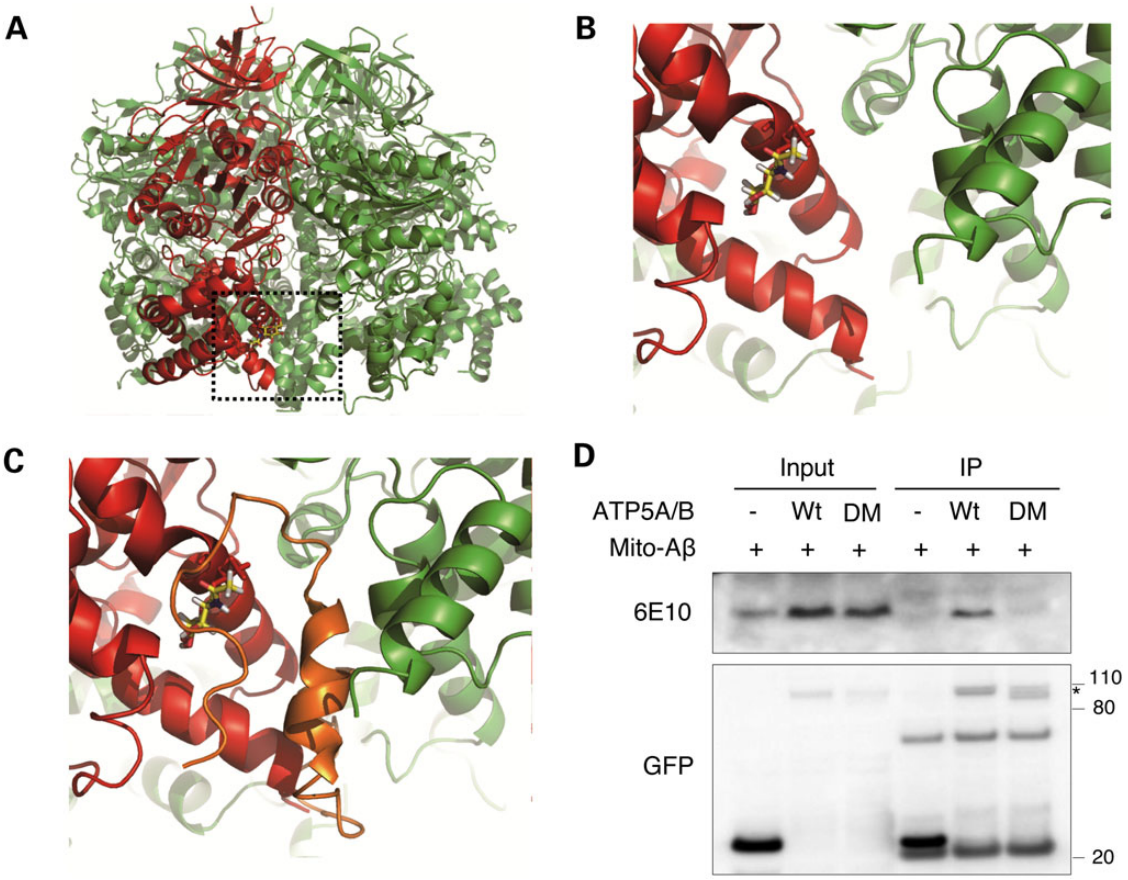

Figure 6. Binding of Aβ to ATP synthase. (**A**) Overall view of glycosylated ATP synthase complex. *O*-GlcNAcylation of ATP5A (red) on Thr432 is shown as a stick model. The neighboring β subunit (ATP5B) is colored in green. (**B**) Enlarged view of the *O*-GlcNAcylation site. (**C**) Molecular docking simulation between ATP synthase and Aβ. ATP5A, red; ATP5B, green; Aβ, orange. (**D**) Validation of Aβ binding on ATP synthase. Cells were transfected with control GFP vector or GFP-tagged WT or deletion mutant ATP5A/B (DM) in combination with mitochondria-targeted Aβ (mito-Aβ). After 48 h transfection, whole cell lysates were prepared and immunoprecipitated with anti-GFP antibody. The co-immunoprecipitated Aβ was detected with anti-Aβ mAb (6E10). Star indicates overexpressed protein.

modification of proteins that could provide a possible mechanism for modulating ATP synthase activity. This assumption is supported by the existence of a mitochondrial isoform of OGT (mOGT). Indeed, recent two reports using mass spectrometry have revealed evidence that ATP5A and/or ATP5B could be *O*-GlcNAcylated (35,36). In these reports, however, it was not confirmed whether the modification of subunits affects the activity of the whole enzyme complex.

In our present study, ATP5A was found to be *O*-GlcNAcylated on Thr432 residue and the level of ATP5A *O*-GlcNAcylation was reduced in AD human tissue and AD mouse model. Based on this observation, we found that regulation of the *O*-GlcNAcyl modification using chemical inhibitors or genetic modulation affected ATP synthase activity and the production of ATP. Furthermore, extracellular Aβ reported to be imported into the mitochondrial matrix as previous study (37) bound directly with the ATP synthase in close proximity to the *O*-GlcNAcylation site of ATP5A (Fig. 6). The interaction between Aβ and the alpha subunit of ATP synthase hampered the binding of mOGT on its recognition site in pathological condition, resulting in decreased ATP synthase activity and ATP production in AD (Fig. 8).

Interestingly, in spite of the presence of mOGT, only a few reports have considered the *O*-GlcNAcylation of mitochondrial proteins and most of them have just reported evidence for *O*-GlcNAcylation using a proteomic approach (35,38). None of these studies linked the effects of *O*-GlcNAcylation to the functional modulation of proteins. Here, we showed for the first time that the activity of ATP synthase, which is located in the mitochondrial inner membrane facing the mitochondrial matrix, is modulated by *O*-GlcNAcylation. It is intriguing that our data suggest ATP synthase subunit β (ATP5B) might be also *O*-GlcNAcylated (Supplementary Material, Table S2). The catalytic F1 subunit of ATP synthase, which consist of three α- and three β-subunits, is crucial for regulating its activity (9). The dissociation of the level ATP/ATPase activity from the level of *O*-GlcNAc-ATP5A raises the possibility that *O*-GlcNAcylation of other ATP synthase subunits also have effect on coordinating its function. Their relationships with *O*-GlcNAc-dependent mechanisms deserve further investigation.

On the other hand, to modulate the activity of certain proteins through *O*-GlcNAcylation, cells should be equipped with enzymes that catalyse reactions in both the catabolic and anabolic directions, such as ncOGT and OGA for the *O*-GlcNAcylation of cytosolic proteins and kinases and phosphatases for phosphorylation (39). Our results clearly showed that Aβ treatment significantly down-regulated the *O*-GlcNAcylation of ATP5A (Figs. 3A and 7A) and this effect was rescued by enhanced *O*-GlcNAcylation using ThG treatment (Fig. 7A). These results suggest that the *O*-GlcNAcylation of ATP5A is removed under certain conditions and, in turn, it is restored by up-regulation of *O*-GlcNAcylation. Furthermore, our data showed that pathologically excessive Aβ treatment or

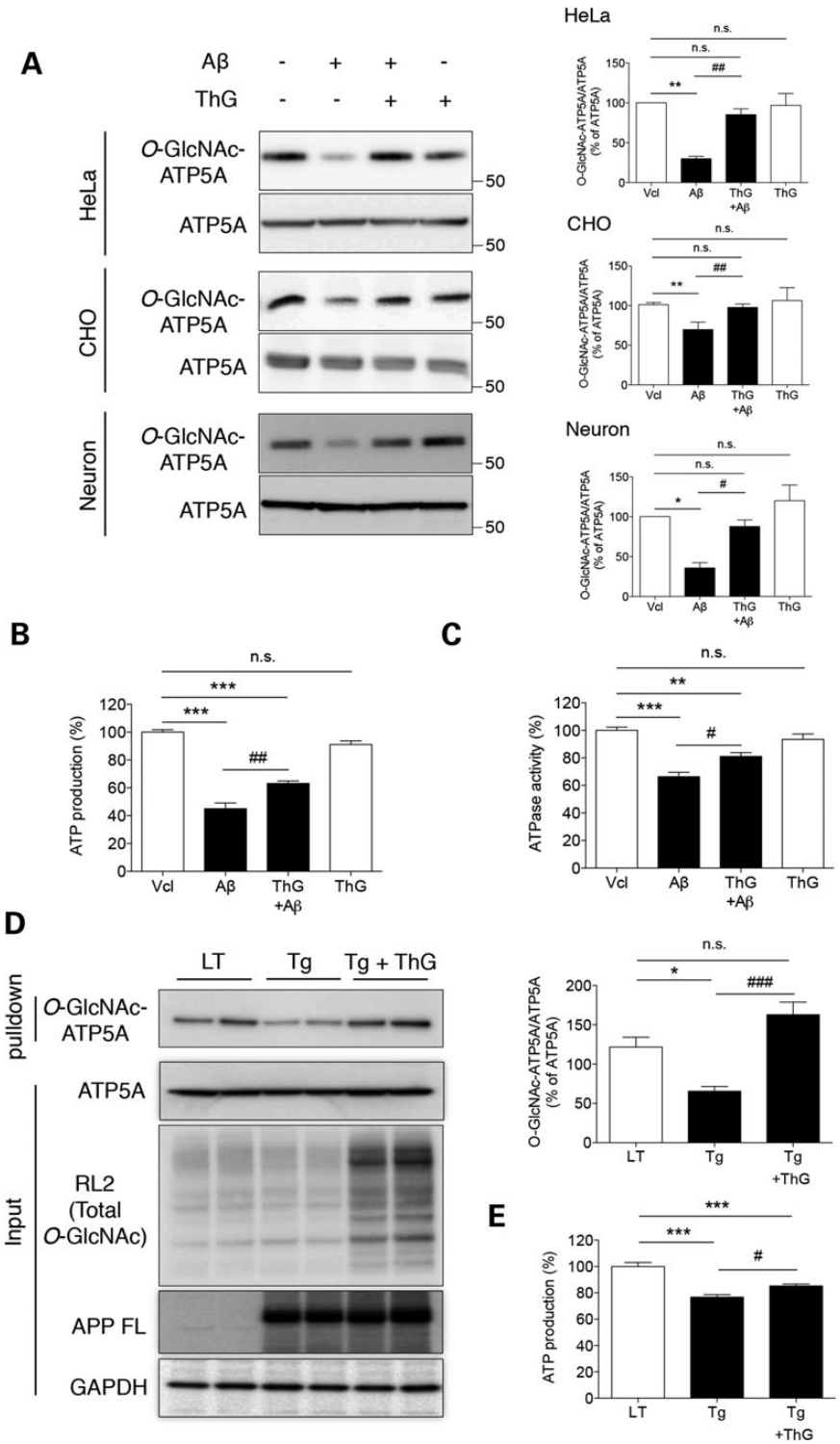

Figure 7. Restoration of impaired ATP5A O-GlcNAcylation by enhanced O-GlcNAcylation. HeLa cells, CHO cells and primary cultured cortical neurons were treated with Aβ (3 μM, 24 h) in the presence or absence of ThG and then whole cell lysates were prepared. The levels of O-GlcNAcylated and total ATP5A (**A**), ATP production (**B**) and ATPase activity (**C**) were measured by western blotting or *in vitro* assays, respectively ($n = 3$ per group). Bar graphs in (A) show densitometric quantification of O-GlcNAcylated ATP5A in each cell. The results were represented as mean ± standard error from three independent experiments. ***$P < 0.001$, **$P < 0.01$ and *$P < 0.05$ versus vehicle (Vcl)-treated; ##$P < 0.01$ and #$P < 0.05$ versus Aβ-treated; n.s.: not significant. (**D**) Total proteins were extracted from the dissected cortices of mice (Littermate + saline, LT; Tg6799 + saline, Tg; Tg6799 + ThG, Tg + ThG) to determine the indicated protein levels. Total O-GlcNAcylated proteins were pulled down with sWGA-agarose beads from cortex lysates and the level of O-GlcNAc-ATP5A was then assessed by western blotting with an anti-ATP5A mAb. Bar graph shows densitometric quantification of O-GlcNAcylated ATP5A ($n = 4$ per group). *$P < 0.05$ versus LT; ###$P < 0.001$ versus Tg; n.s.: not significant. (**E**) ATP production was measured in brain extracts from mice (Littermate + saline, LT; Tg6799 + saline, Tg; Tg6799 + ThG, Tg + ThG) ($n = 4$ per group). The results were represented as mean ± standard error from three independent experiments. ***$P < 0.001$ versus LT; #$P < 0.05$ versus Tg; n.s.: non-significant.

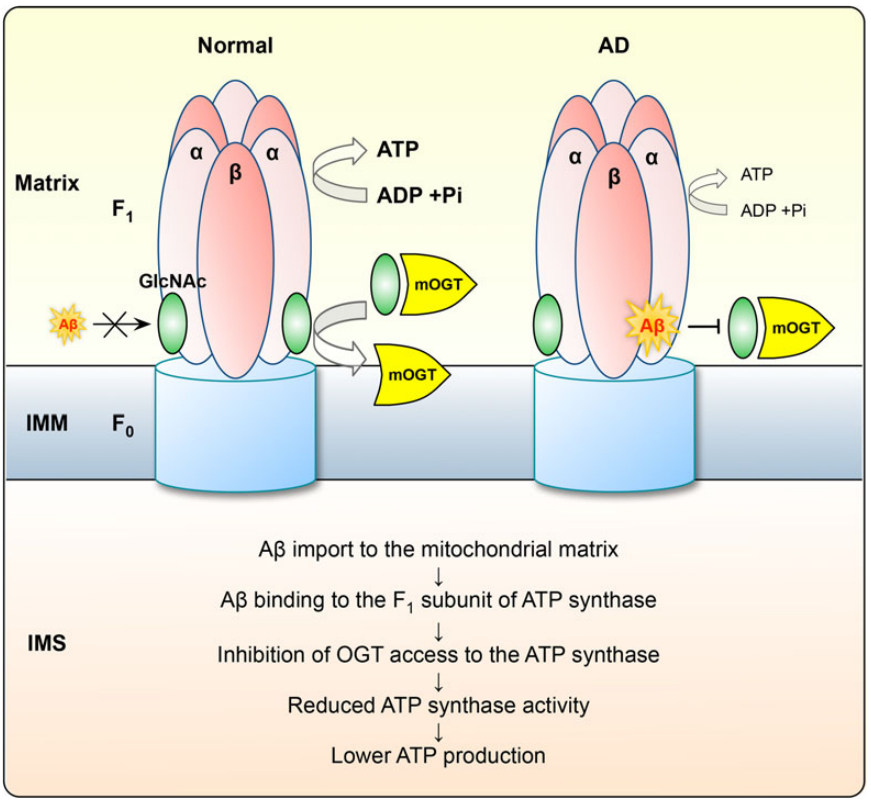

Figure 8. Schematic diagram.

overexpression of the ATP5A T432A mutant inhibited the access of mOGT to ATP5A (Fig. 5). This result indicates that the interaction of mOGT with ATP5A is critical for regulation of ATP5A O-GlcNAcylation in mitochondria. Recently, Hart and his colleagues first identified mitochondrial OGA (mOGA) in cardiac tissue using transmission electron microscopy (TEM) (40). However, the structure and role of mOGA in brain are poorly understood yet. Mechanisms of O-GlcNAc cycling enzyme reaction in mitochondria are still questionable, both Aβ and mOGA may compete with mOGT. It may be that, OGA inhibition possibly can give chance to access more mOGT to ATP5A and thus promotes O-GlcNAcylation. Although our collective data support the predicted model shown in Figure 8, we cannot rule out the precise mechanism how mOGA and Aβ compete with mOGT. Additional detailed studies are required to understand the precise mechanisms involved in regulating O-GlcNAcylation of other mitochondrial proteins.

Another known regulator of ATP synthase activity is inhibitory factor 1 (IF1) (30). Walker *et al.* reported that dimerized IF1 bound to the cleft between the α and β subunits. According to our molecular docking simulation, the binding site of IF1 on ATP synthase does not overlap with the O-GlcNAcylation site, Thr432. However, it is still possible that O-GlcNAcylation induces a conformational change in the IF1 binding cleft. Therefore, it would be interesting to test whether the O-GlcNAcylation of Thr432 affects the binding of IF1 to ATP synthase.

Consistent with our result shown here, the Vocadlo group has suggested a link between O-GlcNAcyl modifications and the pathogenesis of AD. They showed that increased O-GlcNAcylation of Tau could ameliorate the formation of tangles by decreasing phosphorylation of tau (41). Based on these observations, we suggest that the modulation of O-GlcNAcylation can be a way to influence the pathogenesis of AD.

Methods

Animal and human brain samples and intravenous injection

Tg6799 mice overexpressing human amyloid precursor protein (APP) 695 with three familial AD (FAD) mutations (Swedish, Florida and London) and human presenilin 1 (PS1) with two mutations (M146L and L286V) under the transcriptional control of the murine Thy-1 promoter (5X FAD mice) were purchased from Jackson Laboratories (Bar Harbor, ME, USA). Human brain samples were obtained from Mayo clinic, college of medicine (see Supplementary Material, Table S1 for additional information). Seven-month old Tg6799 and littermate B6/SJL mice were used for brain tissue analysis (Oakley *et al.*, 2006). For intravenous injection, 7-month old mice were anesthetized with Zoletil and Rompun mixture (1 ml/kg intraperitoneally). ThG (50 mg/kg) or vehicle was daily administrated into the femoral vein for 2 days.

Cell culture and transfection

HeLa and CHO cells were cultured in Dulbecco's modified Eagles medium (DMEM; HyClone, USA) supplemented with 10% fetal calf serum and penicillin/streptomycin at 37°C under 5% CO_2. For transfection, constructs indicated in the figure legends were mixed with Fugene HD at a 1:3 ratio or Lipofectamine LTX in Opti-MEM (GIBCO-BRL, USA). After 15 min, the mixture was added to the culture and incubated for 48 h. To obtain whole cell lysates, cells were washed twice with cold PBS and then lysed with cold RIPA buffer (Intron Biotechnology, Korea) containing protease inhibitor cocktail (Sigma, USA). The lysates were centrifuged at 16 000 ×*g* for 10 min. The supernatants were used as whole cell lysates.

Primary cortical neuron culture

Wild-type mouse brains were dissected at postnatal day 1 and incubated with trypsin (0.25%, 30 min at 37°C; Sigma, USA). Dissociated neurons were plated on the dishes pre-coated with poly-D-lysine and incubated for 21 days in NeuroBasal medium supplemented with B27 and penicillin/streptomycin.

Chemicals, cDNAs and siRNAs

N-acetylglucosamine and β-hexosaminidase (β-HEX) were purchased from New England Biolabs (USA). Thiamet G and ST045849 were purchased from Sigma (USA) and Timtec (USA), respectively. The cDNA construct for ATP5A-FLAG, ATP5B-FLAG, nucleo/cytosolic OGT (ncOGT) and mOGT was a kind gift from Dr Jin Won Cho of Yonsei University (Seoul, Korea). ATP5A-GFP and ATP5B-GFP constructs were generated using Gateway cloning technology (Invitrogen, USA). The deletion mutant constructs of ATP5A-GFP (Δ 355/405–408) and ATP5B-GFP (Δ 386/394–456) were made using site-directed mutagenesis kit (Enzynomics, Korea) according to the manufacturer's instructions. The siRNAs for OGT were purchased from Bioneer (Korea), with siRNA sequences as follows: sense 5′-GGAGCCUUGCAGUGUUAUA (dTdT)-3′, antisense 5′-UAUAACACUGCAAGGCUCC(dTdT)-3′.

Aβ preparation and treatment

$A\beta_{1\text{-}42}$ peptide purchased from American Peptide was dissolved in hexafluoroisopropanol and lyophilized in a Speedvac (Labconco, USA). The lyophilized peptides were dissolved in dimethylsulfoxide (DMSO) at a final concentration of 1 mM.

Mitochondrial fractionation

For mitochondrial fractionation, cells were harvested with hypotonic buffer [20 mM HEPES (pH 7.6), 220 mM mannitol, 70 mM sucrose, 1 mM EDTA and 0.5 mM phenylmethylsulfonyl fluoride]. After swelling for 15 min on ice, cells were homogenated using 30 strokes of a Dounce homogenizer. Cell homogenates were centrifuged at 800 ×*g* at 4°C for 10 min to remove the nuclear pellet. Mitochondria in the supernatant were pelleted by centrifugation at 10 000 ×*g* at 4°C for 20 min.

sWGA-agarose pull down, immunoprecipitation and western blotting

For immunoprecipitation of GFP-tagged ATP5A, cells were lysed in 1% NP-40 buffer (25 mM Tris–HCL, pH 6.8, 150 mM NaCl, 1 mM EDTA, 5% Glycerol) containing protease inhibitor cocktail (Sigma, USA) and O-GlcNAcase inhibitor (ThG). GFP-tagged proteins were incubated with GFP antibody at 4°C for 12 h and then with protein A/G beads at 4°C for 2 h. For immunoprecipitation of O-GlcNAcylated ATP5A, cells or brain tissues were lysed in RIPA buffer containing protease inhibitor cocktail (Sigma, USA) and O-GlcNAcase inhibitor (ThG). O-GlcNAcylated proteins were pulled down using sWGA-conjugated agarose beads at 4°C for 12 h. In both cases, precipitates were centrifuged, and washed with washing buffer before the beads were re-suspended in SDS-PAGE buffer. Samples were boiled for 5 min, separated in 4–12% Bis-Tris Nu-PAGE gels (Invitrogen, USA) and transferred onto polyvinylidene difluoride (PVDF) membranes. Membranes were blocked with 5% skim milk (Bioworld, USA) for 1 h and then probed with antibodies against the indicated proteins, using monoclonal antibodies against ATP5A (Abcam, UK), RL2 (Abcam, UK), GFP (Abcam, UK), Tom20 (SantaCruz, USA), β-actin (Sigma, USA), 6E10 (Covance, USA) for APP full-length (FL) and C-terminal fragments (CTFs), and polyclonal antibodies against OGT (Sigma, USA), OGA (Sigma, USA), GAPDH (Millipore, Germany), TIMM17b (Abcam, UK).

Measurement of total ATP

Cellular ATP levels were measured using the ATP Determination Kit (Molecular Probes, USA) according to the manufacturer's instructions. A 90-μl aliquot of ATP Determinant Kit reaction solution was added to 10 μl of total cell lysate in a 96-well plate. Plates were agitated for 1 min and luminescence was measured. ATP production was also determined in brain samples from WT and 5XFAD mice, according to the manufacturer's protocol (Abcam, UK). In brief, isolated brains were homogenized with ATP assay buffer; 50 μl of the reaction mix was added to 50 μl of tissue homogenate. ATP production was measured by fluorescence with an excitation wavelength of 535 nm and an emission wavelength of 587 nm.

ATPase activity assay

ATPase activity was measured in HeLa cell homogenates with an ATP synthase Enzyme Activity Microplate Assay Kit (Abcam, UK) according to the manufacturer's instructions. Briefly, 1 μg/μl of each solubilized fraction was loaded into the wells of a microplate pre-coated with monoclonal anti-ATP synthase antibody. A 40-μl aliquot of Lipid mix was added to each well after 3 h incubation at room temperature (RT). Plates were incubated for 45 min at RT and an equal volume of reagent mix was added. The ATPase activity rate was measured as the change in absorbance at 340 nm over 2 h.

O-GlcNAcylated peptide enrichment and mass spectrometry analysis

The O-GlcNAc sites were analyzed using a mass spectrometer as previously described (42). Briefly, proteins isolated from the dissected cortices of Tg6799 mice or LTs were dissolved in 8 M urea and reduced with 10 mM DTT for 1 h at RT, followed by alkylation with 30 mM iodoacetamide for 30 min at RT in the dark. Proteins were incubated with sequencing grade-modified trypsin (Promega, USA) overnight at 37°C. Peptides were desalted using a C18 Sep-Pak cartridge (Waters Corp., USA). The digested samples were resuspended in 25% acetic acid and subjected to separation of O-GlcNAcylated and phosphorylated peptides using a TiO2 affinity column. O-GlcNAcylated peptide fractions were further subjected to β-Elimination/Michael Addition with DTT (BEMAD). The DTT-modified samples were enriched using thiopropyl sepharose 6B beads (GE HealthCare Life Sciences, UK) for further analysis.

The peptides were dissolved in 50 μl solvent A [2% acetonitrile (ACN), 0.1% formic acid (FA) in H_2O], and 5 μl of the sample was analyzed by MS using a C18 column with a 2–38% gradient of solvent B (98% ACN, 0.1% FA in H_2O) for 90 min at a flow rate of 300 nl/min (43). MS data were recorded on an LTQ Orbitrap (Thermo Fisher Scientific, USA) interfaced with a nano-HPLC system (Easy nLC, Thermo Fisher Scientific, USA). Tandem mass spectra (MS/MS) were analyzed using the Sorcerer-SEQUEST search program. UniProt was used for database searching with carbamidomethyl (C) as a fixed modification and parameters set for oxidation of methionine and DTT-derivatized peptides, including mass increases of 136.25 Da (DTT) for serine and threonine.

Molecular dynamics simulation and molecular docking simulation

Molecular dynamics simulations of the GlcNAcylated ATP synthase complex were performed using CHARMM (44). The starting structure for the ATP synthase complex was based on the X-ray structure (PDB ID: 1OHH) (30). After the irrelevant ligand was omitted from this structure, the carbohydrate O-GlcNAc was anchored at the Thr432 residue on the α subunit of the ATP synthase complex using the PATCH command in CHARMM. The CHARMM36 force field was used to parameterize all atoms of the ATP synthase complex and the bound GlcNAc moiety. This system was minimized in vacuum using the 100 steps of steepest descent (SD) method, followed by 1000 steps of the adopted basis Newton–Raphson (ABNR) method with 0.01 kcal/mol tolerance gradients. The solvated system was constructed using periodic boundary conditions with an octahedral water box, in which balanced ion molecules were added to neutralize the system, and the Particle Mesh Ewald method was used for computing long-range electrostatic interactions. The number of grid points for the charge mesh and the κ value were 150 and 0.34, respectively. After simple SD and ABNR minimization with 50 steps, the system was heated from 110 to 310 K for 10 000 steps with 1-femtosecond (fs) time steps. The bond lengths of all atoms were constrained by the SHAKE command, and the non-bonded interactions were truncated with a 16-Å cutoff. The system was equilibrated at a constant 310 K for 120 picoseconds with 1 fs time steps. The temperature and pressure of the system were regulated using Hoover's thermostat and the pressure piston method, respectively. All subunits of the ATP synthase complex and Aβ (PDB ID: 2LFM) structures were submitted to the ClusPro 2.0 protein-protein docking server as receptor and ligand, respectively (45). The default parameters were used for the fast rigid-body docking algorithm. The top 10 structures based on balanced scores were chosen to compare the results of MD simulations.

Statistical analysis

The results were analyzed by unpaired *t*-tests or one-way analysis of variance (ANOVA) with Bonferroni post-hoc tests for multiple comparisons ($^{*}P < 0.05$, $^{**}P < 0.01$, $^{***}P < 0.001$ versus vehicle-treated sample; $\#P < 0.05$, $\#\#P < 0.01$, $\#\#\#P < 0.001$ versus treated sample).

Supplementary Material

Supplementary Material is available at *HMG* online.

Conflict of Interest statement: All authors report no financial interests or potential conflicts of interest. The data contained in the manuscript currently being submitted have not been published previously. The animals were treated and maintained as per the Guide for the Care and Use of Laboratory Animals (NIH publication No. 85–23, revised 1985), and the Animal Care and Use Guidelines of Seoul National University, Seoul, Korea. All experiments were approved by the Institute of Laboratory Animal Resources of Seoul National University. We made an effort to minimize the numbers and suffering of the animals used in the experiments. All authors have reviewed the content of the manuscript being submitted, approved of its content and validated the accuracy of the data.

Funding

This work was supported by grants from the National Research Foundation [2015R1A2A1A05001794, 2014M3C7A1046047, 2015M3C7A1028790 and the Medical Research Center (2011-0030738)]; the KIST Institutional Program (2E24242-13-135) and Protein metabolism medical research center through Seoul National University Nobel Laureates Invitation program for I. M.-J.; Brain Korea 21 Plus program for S.M.J. and I. M.-J.; NRF-2013R1A2A1A01008067 for J.W.C. and from GHR Foundation (JK), NIH AG016574 (D.W.D., M.E.M. and J.K.), Jacoby Professorship of Alzheimer Research (D.W.D), Donors Cure Foundation (M.E.M.) and Einstein Aging Study (NIH P01-AG03949) (D.W.D).

References

1. Ittner, L.M. and Gotz, J. (2011) Amyloid-beta and tau–a toxic pas de deux in Alzheimer's disease. *Nat. Rev. Neurosci.*, **12**, 65–72.
2. Chabrier, M.A., Blurton-Jones, M., Agazaryan, A.A., Nerhus, J.L., Martinez-Coria, H. and LaFerla, F.M. (2012) Soluble abeta promotes wild-type tau pathology in vivo. *J. Neurosci.*, **32**, 17345–17350.
3. Spires-Jones, T.L. and Hyman, B.T. (2014) The intersection of amyloid beta and tau at synapses in Alzheimer's disease. *Neuron*, **82**, 756–771.
4. Rowe, C.C., Ng, S., Ackermann, U., Gong, S.J., Pike, K., Savage, G., Cowie, T.F., Dickinson, K.L., Maruff, P., Darby, D. *et al.* (2007) Imaging beta-amyloid burden in aging and dementia. *Neurology*, **68**, 1718–1725.
5. Chan, D.C. (2006) Mitochondria: dynamic organelles in disease, aging, and development. *Cell*, **125**, 1241–1252.
6. Koopman, W.J., Nijtmans, L.G., Dieteren, C.E., Roestenberg, P., Valsecchi, F., Smeitink, J.A. and Willems, P.H. (2010) Mammalian mitochondrial complex I: biogenesis, regulation, and reactive oxygen species generation. *Antioxidants & Redox Signaling*, **12**, 1431–1470.
7. Habersetzer, J., Ziani, W., Larrieu, I., Stines-Chaumeil, C., Giraud, M.F., Brethes, D., Dautant, A. and Paumard, P. (2013) ATP synthase oligomerization: from the enzyme models to the mitochondrial morphology. *Int. J. Biochem. Cell Biol.*, **45**, 99–105.
8. Martinez-Reyes, I. and Cuezva, J.M. (2014) The H(+)-ATP synthase: a gate to ROS-mediated cell death or cell survival. *Biochim. Biophys. Acta*, **1837**, 1099–1112.
9. Yoshida, M., Muneyuki, E. and Hisabori, T. (2001) ATP synthase—a marvellous rotary engine of the cell. *Nat. Rev. Mol. Cell Biol.*, **2**, 669–677.
10. Gibson, G.E., Sheu, K.F. and Blass, J.P. (1998) Abnormalities of mitochondrial enzymes in Alzheimer disease. *J. Neural Transm.*, **105**, 855–870.
11. Baloyannis, S.J. (2006) Mitochondrial alterations in Alzheimer's disease. *J. Alzheimers Dis.*, **9**, 119–126.
12. Tillement, L., Lecanu, L. and Papadopoulos, V. (2011) Alzheimer's disease: effects of beta-amyloid on mitochondria. *Mitochondrion*, **11**, 13–21.
13. Dumont, M., Stack, C., Elipenahli, C., Jainuddin, S., Gerges, M., Starkova, N.N., Yang, L., Starkov, A.A. and Beal, F. (2011) Behavioral deficit, oxidative stress, and mitochondrial dysfunction precede tau pathology in P301S transgenic mice. *FASEB J.*, **25**, 4063–4072.
14. Edison, P., Archer, H.A., Hinz, R., Hammers, A., Pavese, N., Tai, Y.F., Hotton, G., Cutler, D., Fox, N., Kennedy, A. *et al.* (2007) Amyloid, hypometabolism, and cognition in Alzheimer disease: an [11C]PIB and [18F]FDG PET study. *Neurology*, **68**, 501–508.
15. Ikonomovic, M.D., Klunk, W.E., Abrahamson, E.E., Mathis, C.A., Price, J.C., Tsopelas, N.D., Lopresti, B.J., Ziolko, S., Bi, W., Paljug, W.R. *et al.* (2008) Post-mortem correlates of in vivo PiB-PET

amyloid imaging in a typical case of Alzheimer's disease. *Brain*, **131**, 1630–1645.
16. Rhein, V., Song, X., Wiesner, A., Ittner, L.M., Baysang, G., Meier, F., Ozmen, L., Bluethmann, H., Drose, S., Brandt, U. *et al.* (2009) Amyloid-beta and tau synergistically impair the oxidative phosphorylation system in triple transgenic Alzheimer's disease mice. *Proc. Natl. Acad. Sci. USA*, **106**, 20057–20062.
17. Terni, B., Boada, J., Portero-Otin, M., Pamplona, R. and Ferrer, I. (2010) Mitochondrial ATP-synthase in the entorhinal cortex is a target of oxidative stress at stages I/II of Alzheimer's disease pathology. *Brain Pathol*, **20**, 222–233.
18. Shaw, L.M., Vanderstichele, H., Knapik-Czajka, M., Clark, C.M., Aisen, P.S., Petersen, R.C., Blennow, K., Soares, H., Simon, A., Lewczuk, P. *et al.* (2009) Cerebrospinal fluid biomarker signature in Alzheimer's disease neuroimaging initiative subjects. *Ann. Neurol.*, **65**, 403–413.
19. Buerger, K., Ewers, M., Pirttila, T., Zinkowski, R., Alafuzoff, I., Teipel, S.J., DeBernardis, J., Kerkman, D., McCulloch, C., Soininen, H. *et al.* (2006) CSF phosphorylated tau protein correlates with neocortical neurofibrillary pathology in Alzheimer's disease. *Brain*, **129**, 3035–3041.
20. Du, H., Guo, L., Fang, F., Chen, D., Sosunov, A.A., McKhann, G.M., Yan, Y., Wang, C., Zhang, H., Molkentin, J.D. *et al.* (2008) Cyclophilin D deficiency attenuates mitochondrial and neuronal perturbation and ameliorates learning and memory in Alzheimer's disease. *Nat. Med.*, **14**, 1097–1105.
21. Lustbader, J.W., Cirilli, M., Lin, C., Xu, H.W., Takuma, K., Wang, N., Caspersen, C., Chen, X., Pollak, S., Chaney, M. *et al.* (2004) ABAD directly links Abeta to mitochondrial toxicity in Alzheimer's disease. *Science*, **304**, 448–452.
22. Hanover, J.A., Krause, M.W. and Love, D.C. (2012) Bittersweet memories: linking metabolism to epigenetics through O-GlcNAcylation. *Nat. Rev. Mol. Cell Biol.*, **13**, 312–321.
23. Zachara, N.E. and Hart, G.W. (2006) Cell signaling, the essential role of O-GlcNAc! *Biochim. Biophys. Acta*, **1761**, 599–617.
24. Hart, G.W., Slawson, C., Ramirez-Correa, G. and Lagerlof, O. (2011) Cross talk between O-GlcNAcylation and phosphorylation: roles in signaling, transcription, and chronic disease. *Annu. Rev. Biochem.*, **80**, 825–858.
25. Butkinaree, C., Park, K. and Hart, G.W. (2010) O-linked beta-N-acetylglucosamine (O-GlcNAc): extensive crosstalk with phosphorylation to regulate signaling and transcription in response to nutrients and stress. *Biochim. Biophys. Acta*, **1800**, 96–106.
26. Kim, C., Nam, D.W., Park, S.Y., Song, H., Hong, H.S., Boo, J.H., Jung, E.S., Kim, Y., Baek, J.Y., Kim, K.S. *et al.* (2013) O-linked beta-N-acetylglucosaminidase inhibitor attenuates beta-amyloid plaque and rescues memory impairment. *Neurobiol. Aging*, **34**, 275–285.
27. Liu, F., Shi, J., Tanimukai, H., Gu, J., Grundke-Iqbal, I., Iqbal, K. and Gong, C.X. (2009) Reduced O-GlcNAcylation links lower brain glucose metabolism and tau pathology in Alzheimer's disease. *Brain*, **132**, 1820–1832.
28. Jacobsen, K.T. and Iverfeldt, K. (2011) O-GlcNAcylation increases non-amyloidogenic processing of the amyloid-beta precursor protein (APP). *Biochemical and Biophysical Research Communications*, **404**, 882–886.
29. Zachara, N.E., Vosseller, K. and Hart, G.W. (2011) Detection and analysis of proteins modified by O-linked N-acetylglucosamine. In Coligan, J.E. [et al.], Current Protocols in Protein Science/Editorial Board, Chapter 12, Unit12 18. John Wiley & Sons, NJ, USA.
30. Cabezon, E., Montgomery, M.G., Leslie, A.G. and Walker, J.E. (2003) The structure of bovine F1-ATPase in complex with its regulatory protein IF1. *Nat. Struct. Biol.*, **10**, 744–750.
31. Cha, M.Y., Han, S.H., Son, S.M., Hong, H.S., Choi, Y.J., Byun, J. and Mook-Jung, I. (2012) Mitochondria-specific accumulation of amyloid beta induces mitochondrial dysfunction leading to apoptotic cell death. *PLoS One*, **7**, e34929.
32. Anello, M., Spampinato, D., Piro, S., Purrello, F. and Rabuazzo, A.M. (2004) Glucosamine-induced alterations of mitochondrial function in pancreatic beta-cells: possible role of protein glycosylation. *Am. J. Physiol. Endocrinol. Metab.*, **287**, E602–E608.
33. Kane, L.A., Youngman, M.J., Jensen, R.E. and Van Eyk, J.E. (2010) Phosphorylation of the F(1)F(o) ATP synthase beta subunit: functional and structural consequences assessed in a model system. *Circ. Res.*, **106**, 504–513.
34. Reinders, J., Wagner, K., Zahedi, R.P., Stojanovski, D., Eyrich, B., van der Laan, M., Rehling, P., Sickmann, A., Pfanner, N. and Meisinger, C. (2007) Profiling phosphoproteins of yeast mitochondria reveals a role of phosphorylation in assembly of the ATP synthase. *Mol. Cell. Proteomics*, **6**, 1896–1906.
35. Park, J., Kwon, H., Kang, Y. and Kim, Y. (2007) Proteomic analysis of O-GlcNAc modifications derived from streptozotocin and glucosamine induced beta-cell apoptosis. *J. Biochem. Mol. Biol.*, **40**, 1058–1068.
36. Cao, W., Cao, J., Huang, J., Yao, J., Yan, G., Xu, H. and Yang, P. (2013) Discovery and confirmation of O-GlcNAcylated proteins in rat liver mitochondria by combination of mass spectrometry and immunological methods. *PLoS One*, **8**, e76399.
37. Hansson Petersen, C.A., Alikhani, N., Behbahani, H., Wiehager, B., Pavlov, P.F., Alafuzoff, I., Leinonen, V., Ito, A., Winblad, B., Glaser, E. *et al.* (2008) The amyloid beta-peptide is imported into mitochondria via the TOM import machinery and localized to mitochondrial cristae. *Proc. Natl. Acad. Sci. USA*, **105**, 13145–13150.
38. Diraison, F., Hayward, K., Sanders, K.L., Brozzi, F., Lajus, S., Hancock, J., Francis, J.E., Ainscow, E., Bommer, U.A., Molnar, E. *et al.* (2011) Translationally controlled tumour protein (TCTP) is a novel glucose-regulated protein that is important for survival of pancreatic beta cells. *Diabetologia*, **54**, 368–379.
39. Hurtado-Guerrero, R., Dorfmueller, H.C. and van Aalten, D.M. (2008) Molecular mechanisms of O-GlcNAcylation. *Curr. Opin. Struct. Biol.*, **18**, 551–557.
40. Banerjee, P.S., Ma, J. and Hart, G.W. (2015) Diabetes-associated dysregulation of O-GlcNAcylation in rat cardiac mitochondria. *Proc. Natl. Acad. Sci. USA*, **112**, 6050–6055.
41. Yuzwa, S.A., Shan, X., Macauley, M.S., Clark, T., Skorobogatko, Y., Vosseller, K. and Vocadlo, D.J. (2012) Increasing O-GlcNAc slows neurodegeneration and stabilizes tau against aggregation. *Nat. Chem. Biol.*, **8**, 393–399.
42. Kang, M.J., Kim, C., Jeong, H., Cho, B.K., Ryou, A.L., Hwang, D., Mook-Jung, I. and Yi, E.C. (2013) Synapsin-1 and tau reciprocal O-GlcNAcylation and phosphorylation sites in mouse brain synaptosomes. *Exp. Mol. Med.*, **45**, e29.
43. Yi, E.C., Lee, H., Aebersold, R. and Goodlett, D.R. (2003) A microcapillary trap cartridge-microcapillary high-performance liquid chromatography electrospray ionization emitter device capable of peptide tandem mass spectrometry at the attomole level on an ion trap mass spectrometer with automated routine operation. *Rapid Commun. Mass Spectrom.*, **17**, 2093–2098.
44. Brooks, B.R., Brooks, C.L. 3rd, Mackerell, A.D. Jr, Nilsson, L., Petrella, R.J., Roux, B., Won, Y., Archontis, G., Bartels, C., Boresch, S. *et al.* (2009) CHARMM: the biomolecular simulation program. *J. Comput. Chem.*, **30**, 1545–1614.
45. Comeau, S.R., Gatchell, D.W., Vajda, S. and Camacho, C.J. (2004) ClusPro: a fully automated algorithm for protein-protein docking. *Nucleic Acids Res.*, **32**, W96–W99.